

An Analysis of Low-Latitude Ionospheric Scintillation and Its Effects on Precise Point Positioning

Rui Xu¹, Zhizhao Liu¹(✉), Min Li^{1,2}, Yu Morton³ and Wu Chen¹

¹Department of Land Surveying and Geo-Informatics, The Hong Kong Polytechnic University, Hong Kong, China

²GNSS Research Center, Wuhan University, Wuhan, Hubei, China

³Department of Electrical and Computer Engineering, Miami University, Ohio, USA

Abstract:

Global Positioning System (GPS) receivers at low latitudes have a high probability of experiencing severe ionospheric scintillations. This paper presents the results of scintillation characteristics and scintillation effect on GPS precise point positioning (PPP), using the data observed by the first ever GNSS scintillation monitoring receiver in Hong Kong. Ionospheric scintillation data were collected in July and August 2012 using a Septentrio PolaRxS Pro receiver located at a station (22°12'N, 114°15'E) in the south of Hong Kong. It was observed that August had much more and stronger scintillations than July in Hong Kong. Amplitude scintillation events ($S_4 \geq 0.4$) were frequently observed during 21:00-3:00 LT (UT+8 hour) in July and 20:00-4:00 LT in August. Strong scintillations ($S_4 \geq 0.8$ or $\sigma_\phi \geq 0.8 \text{ rad}$) were mostly observed during 0:00-1:00 LT in July and 20:00-23:00 LT in August. The effect of scintillations on GPS positioning was evaluated using a dual-frequency PPP method. It revealed that under the impact of severe ionospheric scintillations ($S_4 \geq 1.0$ and $\sigma_\phi \geq 1.0 \text{ rad}$), the largest PPP error can increase to more than 34 cm in the vertical and more than 20 cm in the horizontal components.

Keywords: Ionosphere Scintillation; Scintillation Monitoring; Amplitude scintillation; Phase scintillation; Precise Point Positioning

1. Introduction

Ionospheric scintillation can lead to rapid phase fluctuations and significant amplitude fading when GPS signal passes through regions of ionosphere with plasma irregularities. The distortions on phase and amplitude are usually referred to as phase scintillation and amplitude scintillation, respectively. The scintillation effect is more serious in high and low latitudes and varies with

geomagnetic and solar activity (Basu et al., 1988). In high latitudes, phase scintillation seems more severe than amplitude scintillation (Aquino et al., 2005; Jiao et al., 2013; Ngwira et al., 2010; Spogli and Alfonsi, 2009). In low latitudes, while both amplitude scintillation and phase scintillation can occur, amplitude scintillation is in general more severe than phase scintillation (Forte, 2012; Gwal et al., 2006).

Both amplitude and phase scintillations can degrade the GPS positioning performance by increasing the tracking error, number of cycle slips and probability of loss of lock. Rapid phase variations due to phase scintillations yield an additional Doppler shift in the GPS signal that is added to the total Doppler shift (Leick, 2004). When the total Doppler shift exceeds the bandwidth of carrier tracking loop, loss of phase lock may occur (Leick, 2004). Amplitude scintillations lead to loss of lock through degrading the carrier-to-noise-ratio (C/N_0) to below the receiver threshold (Chiou et al., 2008; de Oliveira Moraes et al., 2011). Losing signal is a major issue in GPS receiver navigation performance (Aquino et al., 2005; Datta-Barua and Doherty, 2003; Kintner et al., 2007; Phoomchusak et al., 2003). Equatorial scintillation has greater impact on navigation performances (Chen et al., 2007; Dubey et al., 2006; de Oliveira Moraes et al., 2011; Phoomchusak et al., 2003). A moderate amplitude scintillation ($S_4 \approx 0.6$) would cause more than 10 m error in GPS C/A code positioning (Phoomchusak et al., 2003). Severe scintillation ($S_4 > 0.7$) can lead to a 22-m latitude error and 14 m longitude error in C/A code positioning (Dubey et al., 2006). Single-point precise positioning error can reach several meters in vertical and tens of centimeters in horizontal when severe ionospheric scintillation occurs (Moreno et al., 2010).

Located in the geomagnetic equatorial region, GNSS receivers in Hong Kong (geographic 22.3°N, 114.2°E) area often experience strong scintillations. The performance of GPS receiver degrades significantly,

especially in solar maximum (Chen et al., 2007; Gao, 2008). Scintillation events were observed in more than one third time of a year in Hong Kong during solar maximum (2001) (Chen et al., 2007; Gao, 2008). Under strong scintillations, the number of loss of lock in a GPS receiver reached 500 per day. This number was below 50 per day during quiet days. Moreover, measurement noises increased significantly under severe scintillations. The number of incidence having pseudorange measurement noise larger than 3σ of 3-year average increased by above 20 times than that under non-scintillation situations. Phase measurement noise level is also increased by a third of the normal values (Chen et al., 2007; Gao, 2008).

These previous studies in Hong Kong are based on total electron content (TEC), rate of TEC (ROT) and the standard deviation of ROT (ROTI) derived from ordinary GPS measurements (Chen et al., 2007; Gao, 2008). Calculated from L1 and L2 phase measurements, these indices cannot measure the amplitude scintillation directly. The low-frequency data sampling rate (1 Hz or lower) also leads to loss of high-frequency components of phase variations, which likely contain phase scintillation information. In this study, a high-rate (50-Hz) GNSS-based scintillation monitoring receiver is used to study the Hong Kong scintillation events. The 50 Hz scintillation data include carrier phase measurements, accumulated in-phases and quadra-phases from the correlator outputs. The conventional scintillation indices S_4 and σ_ϕ are used to measure the scintillation intensity. To study the scintillation effect on GPS positioning, the GPS data are processed using a Precise Point Positioning (PPP) algorithm to evaluate the positioning error under scintillations. The PPP algorithm is a standalone positioning technique using dual-frequency code and phase observations. It utilizes precise ephemeris, accurate satellite clock correction, and physical models to provide highly accurate positioning results (Zumberge et al., 1997). The current PPP technique can produce 1 cm positioning accuracy if all types of errors are effectively corrected (Ge et al., 2007). Geodetic Survey Division (GSD) of Natural Resources Canada (NRCan) introduced an on-line Canadian Spatial Reference System-PPP (CSRS-PPP) (Mireault et al., 2008; Tsakiri, 2008). The CSRS-PPP static and kinematic services can provide positioning solutions at 3-4 cm level and 5-10 cm level (Tsakiri, 2008), respectively. Since the static PPP may mask the effect of scintillations, kinematic PPP is used in this study. GPS data from the scintillation monitoring receiver are resampled to 1.0 Hz. The kinematic PPP results during scintillation events can be directly compared with those of quiet times. Thus, the magnitude of scintillation effect on GPS can be studied.

This paper is arranged as below. Section 2 introduces ionospheric scintillation monitoring methods. Section 3

discusses the characteristics of ionospheric scintillation events observed in Hong Kong during July and August 2012. The scintillation effect on PPP is shown in Section 4. The conclusions are given in Section 5.

2. Ionospheric Scintillation Monitoring using GPS Receiver

Ionospheric scintillation causes GPS signal amplitude fading and phase variations. Affected by scintillation, GPS signals at a receiver can be described as (Hegarty et al., 2001)

$$E = Ae^{j\phi} = E_0\delta E = (A_0\delta A)e^{j(\phi_0+\delta\phi)} \quad (1)$$

where $E_0 = A_0e^{j\phi_0}$ represents the nominal received signal (without scintillation) with nominal amplitude A_0 and nominal phase ϕ_0 ; and $\delta E = \delta A e^{j\delta\phi}$ represents the scintillation signal with scintillation amplitude δA and phase $\delta\phi$. The phase $\delta\phi$ is characterized by its standard deviation σ_ϕ , which can be written as:

$$\sigma_\phi = \sqrt{E(\delta\phi^2)} \quad (2)$$

$\delta\phi$ cannot be measured by a GPS receiver directly, but it can be obtained from detrending of phase measurements. $\delta\phi$ is the high-frequency portions of the carrier phase. To remove the low-frequency portions, a high-pass filter with a cutoff frequency of 0.1 Hz can be used (Van Dierendonck and Arbesser-Rastburg, 2001).

The amplitude δA describes the effect of signal amplitude scintillation. The amplitude scintillation is usually represented by index S_4 that can be calculated from GPS signal intensity (SI) as below (Van Dierendonck and Arbesser-Rastburg, 2001):

$$S_4 = \sqrt{S_{4T}^2 - S_{4N_0}^2} = \sqrt{\frac{E(SI^2) - E(SI)^2}{E(SI)^2} - \frac{100}{S/N_0} \left[1 + \frac{500}{19S/N_0} \right]} \quad (3)$$

The S_4 in Eq. (3) is the corrected S_4 . S_{4T} and S_{4N_0} are the total S_4 and the predicted S_4 due to ambient noises, respectively; S/N_0 represents the signal-to-noise density and it can be obtained from a GPS receiver (Van Dierendonck and Arbesser-Rastburg, 2001; Dubey et al., 2006). The signal intensity SI can be calculated from the narrow band power (NBP) and wide band power

(WBP) as below (Van Dierendonck and Arbesser-Rastburg, 2001)

$$SI = \frac{(NBP - WBP)}{(NBP - WBP)_{lpf}} \quad (4)$$

$$NBP = \left(\sum_{k=1}^N i_k \right)^2 + \left(\sum_{k=1}^N q_k \right)^2 \quad (5)$$

$$WBP = \sum_{k=1}^N (i_k^2 + q_k^2)$$

where $(NBP - WBP)_{lpf}$ is the low-frequency portions of the $(NBP - WBP)$ and is obtained from a linear low-pass filter; i_k and q_k represent the 1 kHz in-phase and quadra-phase sampling, respectively; and, N represents the number of i_k or q_k in one coherent integration period T_{coh} .

In this study, $(NBP - WBP)_{lpf}$ is estimated by the average value of $(NBP - WBP)$ over 1 min (Van Dierendonck and Arbesser-Rastburg, 2001), which can be considered as a 60th order low-pass finite impulse response (FIR) filter. This method can mitigate the unstable S_4 . The values of T_{coh} and N are 20 ms and 20, respectively.

The in-phase (I) and quadra-phase (Q) samplings obtained at 50 Hz from a GPS scintillation receiver are average results of 20 i_k and q_k , respectively. To obtain the $(NBP - WBP)$ from the 50-Hz I and Q samplings, we assume $i_k = I + n_{ik}$ and $q_k = Q + n_{qk}$. n_{ik} and n_{qk} represent in-phase and quadra-phase noises, respectively. They are assumed as Gaussian white noise (Crane, 2001). Since n_{ik} and n_{qk} are small and can be ignored when the GPS signal is accurately tracked, NBP and WBP can be written as

$$NBP = \left(\sum_{i=1}^N I \right)^2 + \left(\sum_{i=1}^N Q \right)^2 = N^2(I^2 + Q^2) \quad (6)$$

$$WBP = \sum_{i=1}^N (I^2 + Q^2) = N(I^2 + Q^2)$$

From Eq. (6), the $(NBP - WBP)$ can be calculated as:

$$(NBP - WBP) = N(N - 1)(I^2 + Q^2) \quad (7)$$

The constant coefficient $N(N - 1)$ in $(NBP - WBP)$ cannot be filtered by a linear low-pass filter in $(NBP - WBP)_{lpf}$ but it is cancelled in the SI calculation. The effect of constant coefficient $N(N - 1)$ on S_4 calculation is small and can be ignored (Niu, 2012). Thus, the calculation of $(NBP - WBP)$ can be simplified as $I^2 + Q^2$.

3. Scintillation Observation in Hong Kong

In this study, one Septentrio PolaRxS Pro ionospheric scintillation receiver was installed at Hok Tsui (22°12'34.3"N, 114°15'28.6"E), south of Hong Kong. This receiver can track multi-frequency GPS, GLONASS, Galileo, and SBAS signals but in this paper only the GPS L1 signal is used to study the scintillation characteristics. The receiver outputs both regular GNSS observation data and scintillation data. The observation data, such as carrier phase measurements, pseudorange measurements and C/N_0 , are recorded at 1 Hz sampling rate. To calculate phase scintillation index σ_ϕ , carrier phase measurements are recorded at 50 Hz. The outputs of correlators (in-phases and quadra-phases) are logged at 50 Hz to calculate the amplitude scintillation index S_4 . This paper investigates scintillation characteristics in Hong Kong based on two months of continuous observation of scintillation data collected in July and August 2012. This section analyzes scintillation events in terms of the scintillation intensity, location and occurrence duration.

3.1 Scintillation intensity characteristics in Hong Kong

To study the scintillation characteristics in Hong Kong, we classify scintillation strengths into five levels as shown in Table 1. The classification is based on the value of scintillation index S_4 or σ_ϕ .

Table 1: Case classification for scintillation intensity

Level	S_4 or σ_ϕ (rad)
1	0.2-0.4
2	0.4-0.6
3	0.6-0.8
4	0.8-1.0
5	≥ 1.0

During July and August 2012, there were 15 days during which there are events with amplitude scintillation at level 3+ ($S_4 \geq 0.6$) and 7 days with phase scintillation at level 3+ ($\sigma_\phi \geq 0.6$ rad), as shown in Table 2. The days with phase scintillations at level 3+ were marked with asterisk as shown in Table 2. It was found that the events

with phase scintillations ($\sigma_\phi \geq 0.6$ rad) always had amplitude scintillations ($S_4 \geq 0.6$). However it was not true vice versa. It can be seen that August had more ionosphere scintillations than July. There were 10 days with $S_4 \geq 0.6$ in August but there were only 5 days in July. Particularly at the end of August (26-31 August), Level 3+ scintillation were more frequent and they were observed nearly every day. Meanwhile, it was also observed the scintillations in August were much stronger than those in July. The scintillation events ($S_4 \geq 1.0$ or $\sigma_\phi \geq 1.0$ rad) were observed in 7 days in August but only one day in July. In addition, phase scintillations with $\sigma_\phi > 0.8$ rad were observed 6 days in August.

It should be noted that S_4 was estimated from the previous 1-min long SI data and outputted at every second. 1-Hz S_4 is used in this study because the GPS PPP solutions, to be shown in Section 4, will be estimated every second. The 1-Hz S_4 can thus show detailed relationship between the scintillation intensity and GPS PPP positioning error. Meanwhile, the GNSS data observation cutoff angle was 10 degrees.

Table 2: Scintillation days ($S_4 \geq 0.6$ or $\sigma_\phi \geq 0.6$ rad) in July and August 2012

July	Date	1	2	9	13	30*
	Max. S_4	0.80	0.95	0.75	0.71	2.41
Max. σ_ϕ (rad)	0.17	0.19	0.26	0.20	1.22	
Aug.	Date	3	5	7*	10*	19
	Max. S_4	1.22	0.84	1.06	0.88	0.77
	Max. σ_ϕ (rad)	0.32	0.51	1.34	1.08	0.42
	Date	26*	27*	29	30*	31*
	Max. S_4	1.21	1.24	0.76	1.28	1.08
Max. σ_ϕ (rad)	1.15	1.17	0.06	1.65	1.14	

In order to analyze Hong Kong ionosphere scintillation characteristics, we chose one typical scintillation in July and one in August for detailed analysis. In July, scintillation events of 9 July were chosen. There were many scintillation events of level 3 or higher on this day and their scintillations durations were longer than those in other days. Furthermore, more satellites were affected by scintillations on 9 July than other days. Similarly, scintillation events observed on 31 August were chosen. On 31 August many scintillations of level 5 were observed.

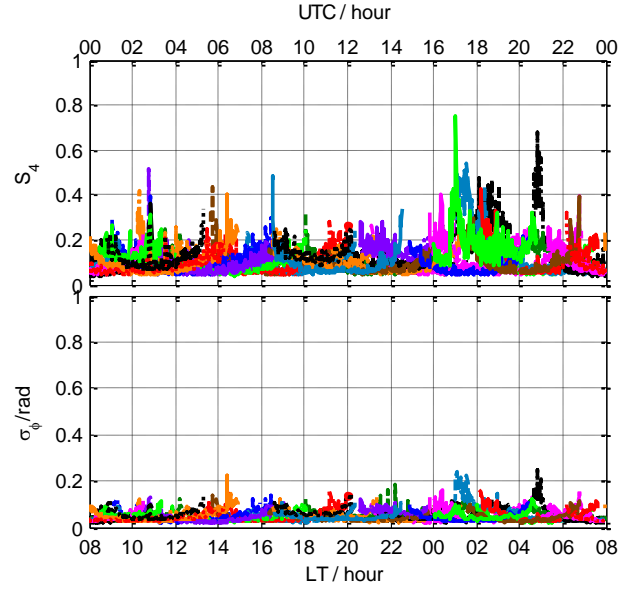


Figure 1: Temporal variations of 1-min S_4 and 1-min σ_ϕ on 9 July 2012

Fig. 1 shows the temporal variations of S_4 and σ_ϕ on 9 July 2012. In Fig.1, the amplitude scintillation occurred during 23:58-05:05 LT (UT+8 hour), lasting 5 hours and 7 minutes. The intensity of the strongest amplitude scintillations reached level 3. They were observed by two satellites: PRN 12 and PRN 29. The highest S_4 was 0.75 observed by PRN 29 at 1:03 LT. The second largest S_4 value 0.68 was observed by PRN 12 at 4:47 LT. Level 2 amplitude scintillations were observed by three satellites: PRN 2, PRN 8 and PRN 21.

From Fig.1, it can also be seen that observed phase scintillation events were much weaker than amplitude scintillation events. During 23:58-05:05 LT, two level 1 phase scintillation events were observed by PRN 8 and PRN 12. The largest σ_ϕ was 0.26 rad observed by PRN 12 at 4:47 LT. The second largest σ_ϕ was 0.24 rad observed by PRN 8 at 1:04 LT.

Fig. 2 shows the temporal variations of S_4 and σ_ϕ on 31 August 2012. The amplitude scintillations were observed during 20:05-1:57 LT, lasting nearly 6 hours. The strongest amplitude scintillation (level 5) with S_4 of 1.08 was observed by satellite PRN 15 at 22:06 LT. Level 4 amplitude scintillations affected 2 satellites: PRN 8 and PRN 12. Level 3+ amplitude scintillations were observed by 10 satellites. The details of amplitude scintillations at level 3+ were shown in Table 3. Level 2 amplitude scintillations were observed by two satellites only: PRN 2 and PRN 26.

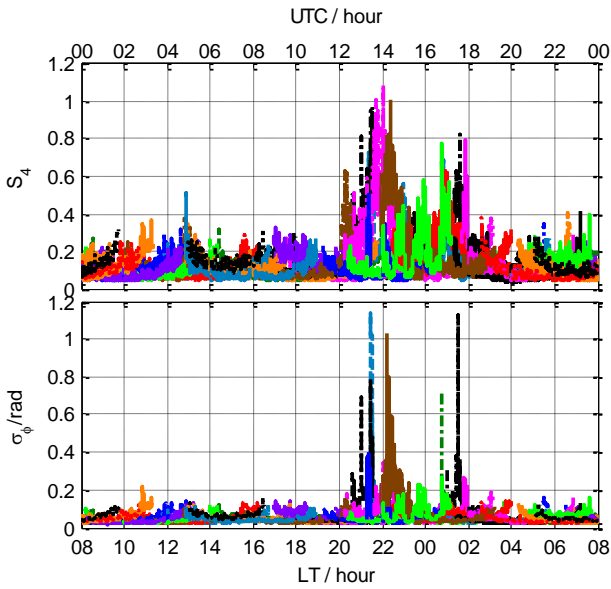


Figure 2: Temporal variations of 1-min S_4 and 1-min σ_ϕ on 31 August 2012

Table 3: Scintillation events (Max. $S_4 \geq 0.6$) on 31 August 2012

Affected Satellites	Scint. Period (LT)	Max. S_4	Max. σ_ϕ (rad)
PRN 08	21:19-21:37	0.87	1.14
PRN 12	20:58-21:34	0.97	0.79
	01:17-01:54	0.82	1.13
PRN 14	00:42-00:52	0.68	0.71
PRN 15	21:24-22:34	1.08	0.38
PRN 17	20:05-20:34	0.63	0.16
PRN 18	00:48-01:02	0.69	0.09
PRN 21	00:47-01:12	0.63	0.13
PRN 25	01:45-01:57	0.79	0.27
PRN 27	21:54-22:40	0.62	1.03
PRN 29	01:02-01:14	0.78	0.26

Phase scintillations were also observed during 20:05-1:57 LT, as shown in Fig. 2. Five phase scintillation events at level 3+ were observed. Three out of them reached level 5. The strongest phase scintillation event was observed by satellite PRN 8 and its maximum value was 1.14 rad at 21:32 LT. The phase scintillations at level 2 were observed by 3 satellites during 20:05-1:57 LT.

Figs. 1 and 2 also show that the phase scintillations were always accompanied by amplitude scintillations. However the amplitude scintillations could occur alone in low-latitudes without phase scintillation. This is consistent with the observation by Gwal et al. (2006). As shown in Fig. 2, the amplitude scintillation observed from PRN 21 reached level 3, but no phase scintillations

was observed (the largest σ_ϕ was only 0.09 rad). In Fig.1, similar situation was found from the scintillation events observed by PRN 12 on 9 July 2012.

3.2 Hourly distribution of observed scintillation events

To analyze the temporal variations of scintillation occurrences, a statistical study of the occurrence of amplitude scintillations and phase scintillations of different levels was conducted. Fig. 3 showed different levels of amplitude scintillations observed in July (a) and August (b). Level 1 amplitude scintillations were observed throughout 24 hours during each day. The number of level 1 amplitude scintillations was several or even tens of times more than that of level 2+ amplitude scintillations. To highlight the occurrence of significant scintillations, level 1 amplitude scintillations were not shown in Fig. 3.

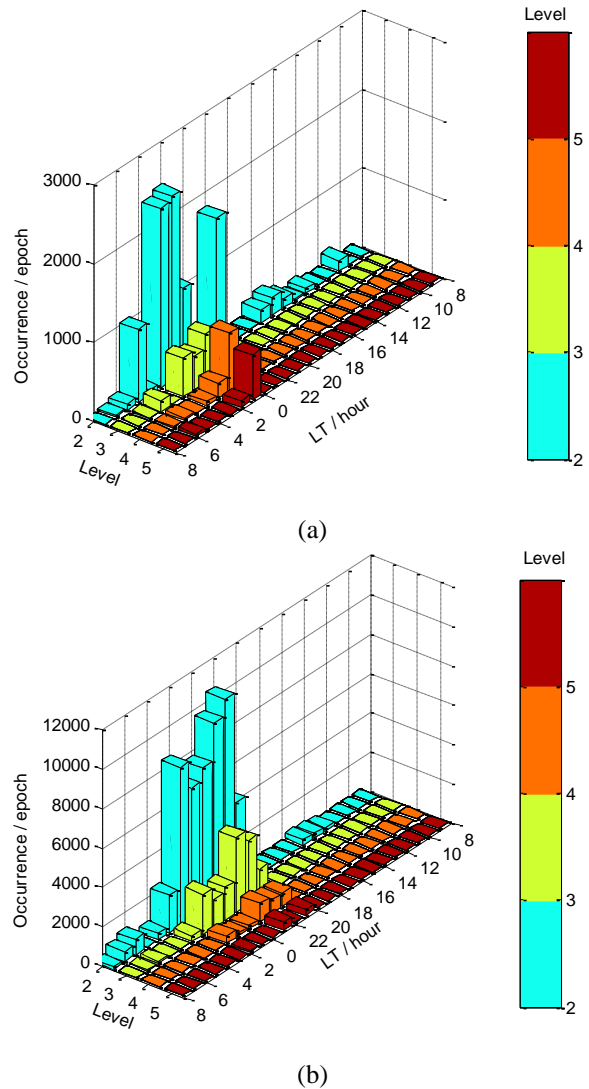


Figure 3: Hourly occurrence of amplitude scintillations ($S_4 > 0.4$) in July (a) and August (b) 2012

In Fig. 3(a), there were 13048 epochs of amplitude scintillation at level 2+. We found that 84.6% of the level 2+ scintillations occurred during 21:00-3:00 LT and 9.5% occurred during 5:00-7:00 LT. Level 3+ amplitude scintillations were primarily observed during 0:00-3:00 LT, which accounted for 89.9% of all the level 3+ amplitude scintillations (3165 epochs). During 0:00-1:00 LT, the highest concentration of level 3+ amplitude scintillation occurred, accounting for 54.6% (1921 epochs) of all the level 3+ amplitude scintillation. The period 0:00-1:00 LT also had the highest concentration of levels 4 and 5 amplitude scintillations. The level 4 and level 5 amplitude scintillations in this hour accounted for 71.5% (738 epochs) and 83.9% (573 epochs) of their categories, respectively.

In Fig. 3(b), the occurrence of level 2+ amplitude scintillations was 67676 epochs. It was observed that 96.7% of level 2+ amplitude scintillations occurred during 20:00-4:00 LT. Level 3+ amplitude scintillations were observed in 17314 epochs, of which 97.4% were observed during 20:00-2:00 LT. Level 4 and level 5 amplitude scintillations were observed in 2923 epochs and 777 epochs, respectively, all of which were observed during 20:00-2:00 LT. Among all the level 4 amplitude scintillations, 78.4% were observed during 20:00-23:00 LT. During the same period, 92.4% of level 5 amplitude scintillations were observed.

Fig. 4 showed different levels of phase scintillations observed in July (a) and August (b) 2012 in Hong Kong. Fig. 4(a) displayed that most phase scintillations were observed during 0:00-2:00 LT, which accounted for 79.6% (1367 epochs) of all the phase scintillations observed. There were 13.2% phase scintillations occurring during 4:00-6:00 LT. During these two periods, amplitude scintillations were also observed as shown in Fig. 3. The observation in Hong Kong confirms that phase scintillations are usually accompanied by amplitude scintillations. For the level 1 phase scintillations, the largest number of hourly occurrences occurred during 1:00-2:00 LT and 682 epochs was observed at level 1. The maximum number of hourly occurrence of level 2+ phase scintillations occurred during 0:00-1:00 LT, in which 404 out of 563 epochs of level 2+ phase scintillations were observed. Coincidentally, most level 4+ amplitude scintillations occurred during the same period 0:00-1:00 LT, as indicated in Fig. 3(a).

Fig. 4(b) showed that more phase scintillations were observed in August. The total number of observed phase scintillations reached 25039 epochs and 94.2% of them occurred during 20:00-2:00 LT. Level 3+ phase scintillations were mainly observed during 20:00-23:00 LT. During this period, the level 4+ amplitude

scintillations had the highest concentration too, as shown in Fig. 3(b).

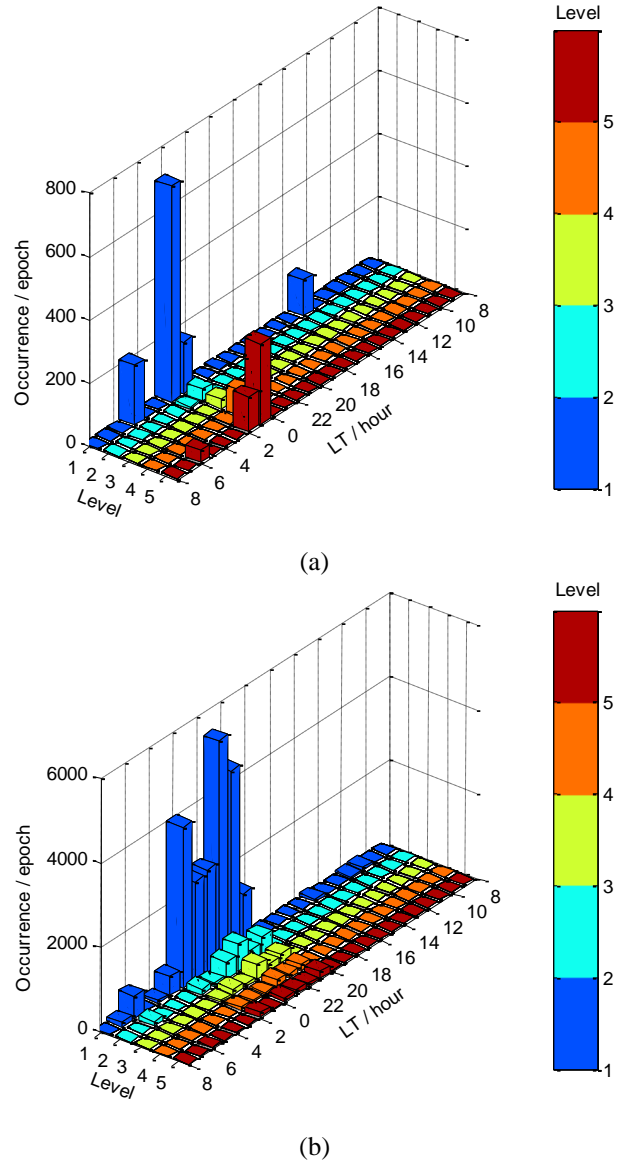


Figure 4: Hourly occurrence of phase scintillations ($\sigma_{\phi} > 0.2$ rad) in July (a) and August (b) 2012

3.3 Spatial distribution of observed scintillation events

Spatial distributions of S_4 index values of different levels observed by all the satellites during July and August 2012 were shown in Fig. 5. The GNSS data observation cutoff angle was 10-degree thus no scintillation was observed below 10-degree.

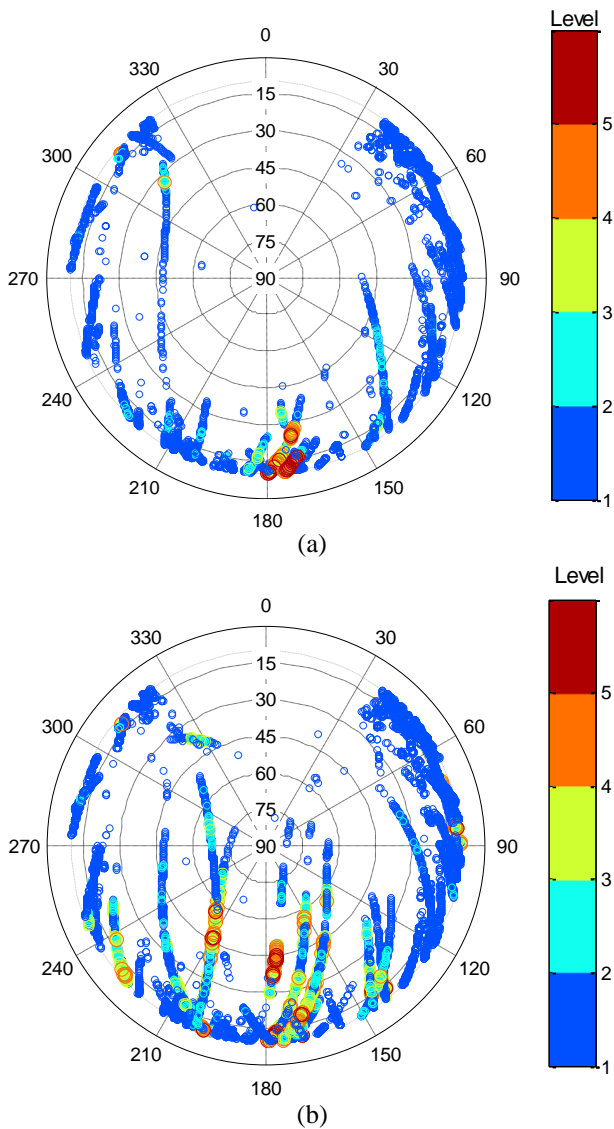


Figure 5: Spatial distribution of different levels of amplitude scintillations observed by all the satellites in July (a) and August (b) 2012

In Fig. 5(a) showed that 95.2% of level 1 amplitude scintillations in July 2012 were observed by satellites below 30-degree elevation angles, with azimuth angle window from 30 to 330-degree. Similarly, 86.6% of level 2+ amplitude scintillations were observed in this area, as shown in Fig. 5(a). More level 2+ amplitude scintillations were observed in the south than in the north. It was found that 92.2% of level 3+ amplitude scintillations concentrated in the region with elevation angle below 30 degrees and azimuth angles within 150-180 degrees.

Fig. 5(b) showed that at higher elevation angles more amplitude scintillations occurred in August than in July. Level 1 amplitude scintillations distributed over almost the whole sky except the area defined by azimuth 330 to

30 degrees and elevation angle below 45 degrees. This phenomenon is associated with the satellite constellation visibility at the GNSS station. In this area, no GPS signal was recorded thus no scintillation event was observed. In Fig. 5(b), stronger amplitude scintillations were observed in the south. Among all the level 2 amplitude scintillations, 89.7% of them were often observed from azimuth 90 to 240 degrees. Fig. 5(b) showed 91.3% of level 3 amplitude scintillations and 94.0% of level 4+ amplitude scintillations were observed from azimuth 120 to 210 degrees.

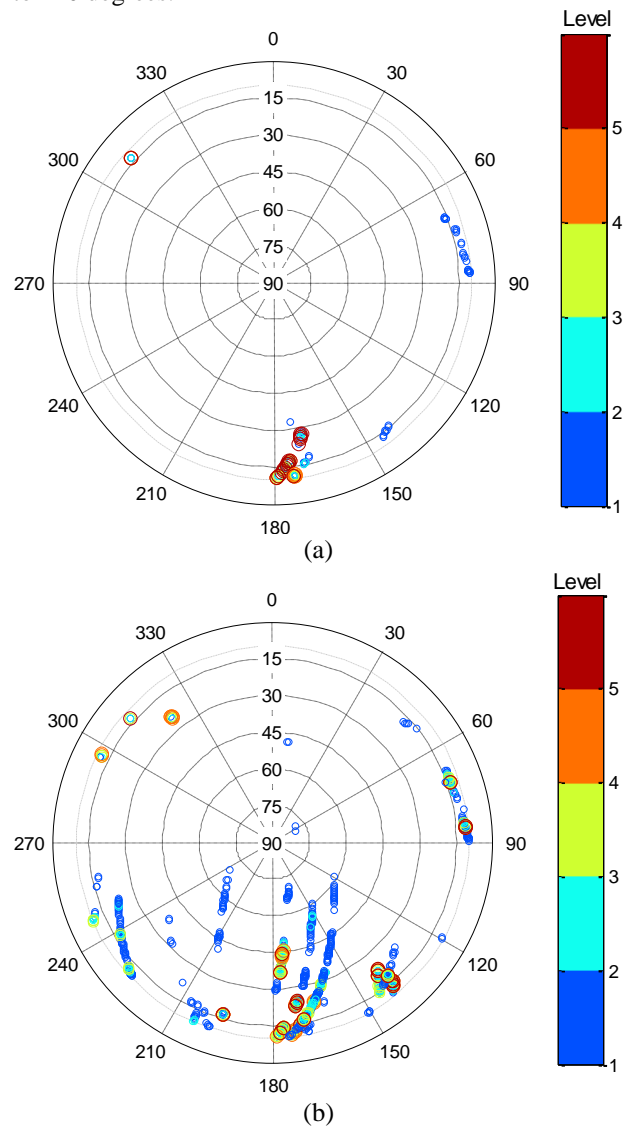


Figure 6: Spatial distribution of different levels of phase scintillations observed by all the satellites in July (a) and August (b) 2012

Fig. 6 showed the spatial distribution of different levels of phase scintillations observed in July (a) and August (b). In Fig. 6(a), phase scintillations were distributed in much smaller areas, compared to amplitude scintillations of the same month shown in Fig. 5(a). In July, 65% of

level 1 phase scintillations were observed by GPS satellites from azimuth 150 to 180 degrees and with elevation below 30-degree. Within the level 1 phase scintillations, 34.4% were observed from azimuth 60-90 degrees. Nearly all level 2+ phase scintillations were observed within the areas of azimuth 150 to 180 degrees and of elevation angle below 30-degree.

In August, as shown in Fig. 6(b), 90.5% of level 1 phase scintillations were observed by satellites with azimuth 120 to 240 degrees and with elevation angle <75 degrees. Above 60% of level 2+ phase scintillation were observed within azimuth 120 to 180 degrees and with elevation angle <60 degrees.

4. Scintillation Effects on GPS Positioning

Moderate and higher levels of ionosphere scintillation frequently occur in low latitudes. The impact of severe scintillations may result in GPS receiver being difficulty providing continuous and reliable positioning results. This section evaluates the effects of low-latitude scintillations on GPS positioning in Hong Kong. A Precise Point Positioning (PPP) algorithm is used as the evaluation tool because the scintillation impact on PPP can be more clearly illustrated than on traditional double-differencing positioning. Based on precise ephemeris, precise satellite clock correction and physical models, the PPP can provide highly accurate positioning results (Zumberge et al., 1997). Thus scintillation effect on PPP will become prominent in the PPP solutions after all other errors have been reduced to a minimum level. In this study, the CSRS-PPP service provided by Natural Resources Canada (NRCAN) was used, in which kinematic service can provide positioning solutions at 5-10 cm level (Tsakiri, 2008). To study the effect of low-latitude scintillation on GPS positioning, we chose two different levels of scintillation event: level 3 scintillation event on 9 July 2012 and level 5 scintillation event on 31 August 2012. The temporal variations of S_4 and σ_ϕ were already shown in Fig. 1 (9 July) and Fig. 2 (31 August). The GPS data were from the Septentrio PolaRxS Pro GNSS scintillation monitoring receiver itself.

Fig. 7 showed the PPP positioning errors in East-North-Up (ENU) coordinates on 9 July. The first two hours (8:00-10:00 LT) were not used in this study considering that PPP needs a long period of time to converge. In Fig. 7, positioning error surges can be found in north and vertical at 4:51 LT. The positioning errors reached -20.8 cm in north and -38.0 cm in vertical. This period was a part of the scintillation period 23:58-5:05 LT (shown in Fig. 1). This error increase was very likely resulted from the level 3 scintillations observed by PRN 12. Excluding the surges, the root mean squares (RMS) of positioning

errors during scintillation period 23:58-5:05 LT in eastern, northern and vertical were 1.2 cm, 1.6 cm and 4.2 cm, respectively. During the period 18:51-23:58 LT (a period of 307 min prior to scintillations), the RMS of positioning error were 1.2 cm in east and north, and 4.0 cm in vertical. It could be seen that the scintillation-caused GPS positioning error surges can considerably degrade the PPP accuracy.

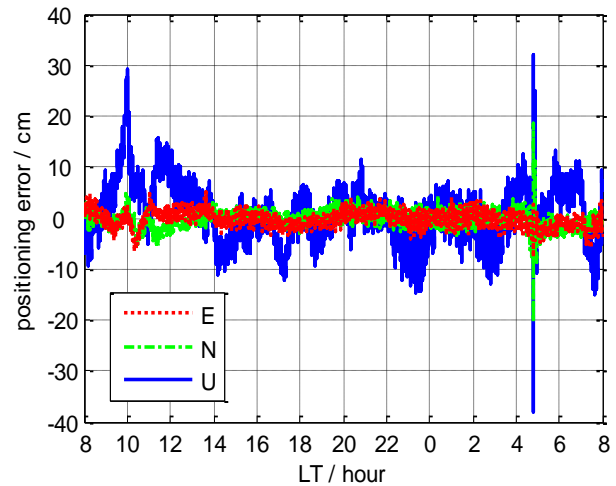


Figure 7: Positioning error on 9 July 2012

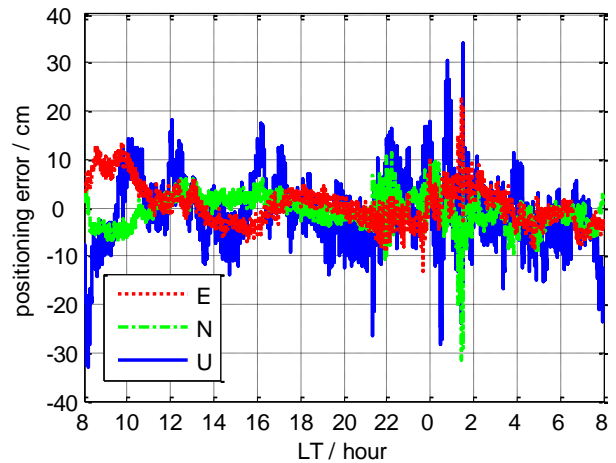


Figure 8: Positioning error on 31 August 2012

Fig. 8 showed PPP positioning errors in East-North-Up (ENU) coordinates for 31 August 2012. Level 5 ionospheric scintillations were observed during 20:05-1:57 LT on that day, as shown in Fig. 2. During this period, significant fluctuations on PPP positioning could be found in Fig. 8. As shown in Fig. 8, the maximum positioning error reached 34.2 cm in vertical, 22.9 cm in east and -31.6 cm in north. RMS of positioning errors were degraded to 7.6 cm in vertical and 3.9 cm in both east and north during scintillation period between 20:05-

1:57 LT. During non-scintillation periods (10:00-20:05 LT and 1:57-8:00 LT), the maximum vertical error was -23.8 cm and the maximum eastern and northern errors were below 15 cm. RMS of positioning errors in east, north and vertical were 3.2 cm, 2.5 cm and 5.4 cm, respectively. It can be seen during the scintillation period RMS errors in all the three components of PPP increased.

To verify that the large fluctuations in Fig. 8 were due to the scintillation, instead of other errors such as satellite clock error, ephemeris error or ionospheric delay, one day of GPS data (29 July 2012) collected under non-scintillation conditions were also processed using the NRCan CSRS-PPP services. Fig. 9 showed the PPP positioning errors under non-scintillation conditions did not have large variations as shown in Fig. 8. The maximum positioning error in east, north and vertical were only -8.7 cm, -5.5 cm and -15.9 cm, respectively. During 20:05-1:57 LT (scintillation period on 31 August 2012), RMS of positioning error were 1.0 cm in east, 1.1 cm in north and 4.0 cm in vertical. Through comparing Fig. 8 and Fig. 9, it could be seen that the significant degradation in PPP positioning accuracy on 31 August was due to ionospheric scintillations, which could cause the receiver frequent loss of tracking of GPS signals. As a result, the satellite geometry might vary abruptly, as shown in Fig. 10 (bottom panel).

Fig. 10 showed the positioning errors for the period of 18:00-2:00 LT (upper panel) and the number of satellites used in PPP and averaged S_4 and σ_ϕ were shown in the bottom panel. The S_4 and σ_ϕ shown in Fig. 10 were mean values of all available satellites. The averaged S_4 increased to above 0.1, in scintillation period. Two significant increments could be found during 21:19-22:35 LT (76 min) and 0:37-1:07 LT (30 min). σ_ϕ increased in these two periods too. The number of satellites varies more dramatically in scintillation periods, especially in 21:19-22:35 LT (76 min) and 0:19-1:43 LT (84 min), compared to the non-scintillation periods. Due to the frequent variations of satellite number, the positioning errors in three directions during 21:19-22:35 LT have larger fluctuations than those during non-scintillation period. The standard deviation (STD) of positioning errors increased to 1.4 cm in east, 2.1 cm in north and 5.8 cm in vertical during 21:19-22:35 LT. During non-scintillation period 18:49-20:05 LT (76 min before scintillation period), STD of positioning errors were 0.9 cm in east, 1.0 cm in north and 3.5 cm in vertical. At 20:19 LT, S_4 increased to 0.26, σ_ϕ increased to 0.10 rad and number of available satellites reduced from 8 to 7. Correspondingly, the positioning error increased to -21.7 cm in vertical and 4.5 cm in north. No increase was observed in the eastern direction.

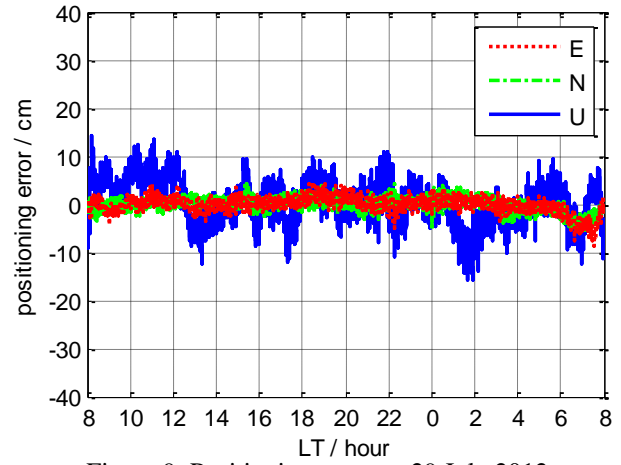


Figure 9: Positioning error on 29 July 2012

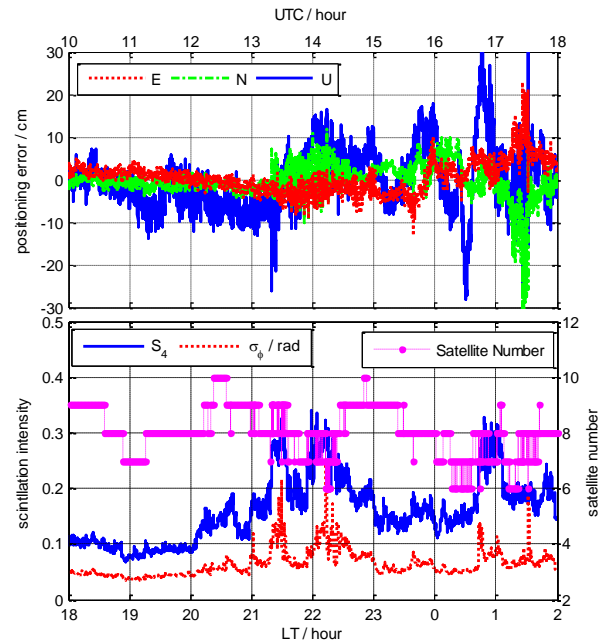


Figure 10: Positioning error, scintillation variations and available satellites during 18:00-2:00 LT on 31 August 2012

The other period with significant S_4 increase was 0:37-1:07 LT. In this period, the STD of positioning errors also increased to 1.9 cm in east, 2.4 cm in north and 8.2 cm in vertical. However, the number of satellites was affected even by weaker scintillations ($S_4 = 0.15-0.2$). During 0:19-1:43 LT, the number of satellites changes 76 times due to ionospheric scintillations. Thus, positioning errors were large during 0:19-1:43 LT. The maximum positioning errors in the three directions occurred at 1:26-1:31 LT. In these moments, the S_4 was 0.18 and σ_ϕ reached 0.19 rad from 0.07 rad.

5. Conclusions

In this study, we analyzed scintillation occurrence in Hong Kong in July and August 2012 based on the data collected from an advanced Septentrio PolaRxS Pro GNSS scintillation monitoring receiver in Hong Kong. Ionospheric scintillations were frequently observed in Hong Kong in both July and August, but August observed much more and stronger scintillations than July. Level 3+ ($S_4 \geq 0.6$ or $\sigma_\phi \geq 0.6$ rad) scintillations were recorded in 10 days in August but only 5 days in July. Compared to phase scintillations, there were considerably more amplitude scintillations in both July and August 2012. In most cases, the phase scintillation values were below 0.2 rad. The level 2+ phase scintillations were often accompanied by amplitude scintillations of $S_4 > 0.6$. However lower level amplitude scintillations often occurred without phase scintillation.

During 21:00-3:00 LT in July of Hong Kong, 84.6% of level 2+ amplitude scintillations were observed. In the same month, 89.9% of level 3+ amplitude scintillation (3165 epochs) occurred 0:00-3:00 LT. During 20:00-4:00 LT in August, 96.7% of level 2+ amplitude scintillations were observed. In August, 97.4% of level 3+ amplitude scintillations were observed during 20:00-2:00 LT.

In July of Hong Kong, 79.6% (1367 epochs) of all levels of phase scintillations occurred during 0:00-2:00 LT. In August, 25039 epochs of all levels of phase scintillations occurred, of which 94.2% occurred during 20:00-2:00 LT. It was observed the majority of level 3+ scintillations in August was observed during 20:00-23:00 LT.

In terms of scintillation distribution, scintillations tend to occur in the south direction. In July, 92.2% of level 3+ amplitude scintillations concentrated in the region with azimuth 150 to 180 degrees and elevation below 30 degrees. In August, 91.3% of level 3 scintillations and 94.0% of level 4+ scintillations were observed within the azimuth zone from 120 to 210 degrees.

The effect of low-latitude scintillation on PPP solution depends on the scintillation intensity. In this study, scintillations can degrade PPP positioning accuracy. A degradation of 38.0 cm in the vertical component was observed when one scintillation occurred on 9 July 2012. On 31 August 2012, one scintillation resulted the PPP vertical component error as large as 34.2 cm. Without scintillations on 31 August 2012, the PPP RMS errors were from 3.2 cm, 2.5 cm and 5.4 cm in east, north and vertical components, respectively. Under the impact of level 5 scintillations on 31 August 2012, the PPP

positioning errors increased to 3.9 cm, 3.9 cm and 7.6 cm in east, north and vertical components, respectively.

Acknowledgments

This research was sponsored by the Hong Kong Polytechnic University project A-PL11 and Hong Kong CERG grant (PolyU 5131/10E). Zhizhao Liu thanks the Program of Introducing Talents of Discipline to Universities (Wuhan University, GNSS Research Center), China. The Natural Resources Canada (NRCan) is thanked for providing the Canadian Spatial Reference System (CSRS) PPP services.

References

- Aquino, M., Moore, T., Dodson, A., Waugh, S., Souter, J. and Rodrigues, F. S. (2005), *Implications of Ionospheric Scintillation for GNSS Users in Northern Europe*, Journal of Navigation, Vol. 58, No. 2, pp. 241–256
- Basu, S., MacKenzie, E. and Basa, S. (1988), *Ionospheric constraints on VHF/UHF communications links during solar maximum and minimum periods*, Radio Science, Vol. 23, No. 3, pp. 363–378
- Chen, W., Gao, S., Hu, C., Chen, Y. and Ding, X. (2007), *Effects of ionospheric disturbances on GPS observation in low latitude area*, GPS Solutions, Vol. 12, No. 1, pp. 33–41
- Chiou, T., Seo, J., Walter, T. and Enge, P. (2008), *Performance of a Doppler-aided GPS navigation system for aviation applications under ionospheric scintillation*, in Proceedings of the 21st International Technical Meeting of the Satellite Division of the Institute of Navigation, pp. 1139–1147, Savannah, GA, USA.
- Crane, R. N. (2001), *A simplified method for deep coupling of GPS and inertial data*, in Proceedings of the 2007 National Technical Meeting of The Institute of Navigation, pp. 311–319, San Diego, CA, USA.
- Datta-Barua, S. and Doherty, P. (2003), *Ionospheric scintillation effects on single and dual frequency GPS positioning*, in Proceedings of ION GPS/GNSS 2003, pp. 336–346, Portland, Oregon, USA.
- Van Dierendonck, A. and Arbesser-Rastburg, B. (2001), *Measuring ionospheric scintillation in the equatorial region over Africa, including measurements from SBAS geostationary satellite signals*, in Proceedings of the 17th International Technical Meeting of the Satellite Division of The

- Institute of Navigation (ION GNSS 2004), pp. 316–323, Salt Lake City, CA, USA.
- Dubey, S., Wahi, R. and Gwal, a. K. (2006), *Ionospheric effects on GPS positioning*, Advances in Space Research, Vol. 38, No. 11, pp. 2478–2484
- Forte, B. (2012), *Analysis of strong ionospheric scintillation events measured by means of GPS signals at low latitudes during disturbed conditions*, Radio Science, Vol. 47, No. 4, pp. RS4009
- Gao, S. (2008), *Monitoring and modelling Hong Kong ionosphere using regional GPS networks*, The Hong Kong Polytechnic University, Hong Kong.
- Ge, M., Gendt, G., Rothacher, M., Shi, C. and Liu, J. (2007), *Resolution of GPS carrier-phase ambiguities in Precise Point Positioning (PPP) with daily observations*, Journal of Geodesy, Vol. 82, No. 7, pp. 389–399
- Gwal, A., Dubey, S., Wahi, R. and Feliziani, A. (2006), *Amplitude and phase scintillation study at Chiang Rai, Thailand*, Advances in Space Research, Vol. 38, No. 11, pp. 2361–2365
- Hegarty, C., El-Arini, M. B., Kim, T. and Ericson, S. (2001), *Scintillation modeling for GPS-Wide Area Augmentation System receivers*, Radio Science, Vol. 36, No. 5, pp. 1221–1231
- Jiao, Y., Morton, Y., Taylor, S. and Pelgrum, W. (2013), *High latitude ionosphere scintillation characterization*, in Proc. ION ITM, San Diego, CA, USA.
- Kintner, P. M., Ledvina, B. M. and De Paula, E. R. (2007), *GPS and ionospheric scintillations*, Space Weather, Vol. 5, No. 9, pp. S09003
- Leick, A. (2004), *GPS satellite surveying*, Wiley.
- Mireault, Y., Tétreault, P., Lahaye, F., Héroux, P. and Kouba, J. (2008), *Online Precise Point Positioning*, GPS World, No. September, pp. 59–64
- Moreno, B., Radicella, S., Lacy, M. C., Herraiz, M. and Rodriguez-Caderot, G. (2010), *On the effects of the ionospheric disturbances on precise point positioning at equatorial latitudes*, GPS Solutions, Vol. 15, No. 4, pp. 381–390
- Ngwira, C. M., McKinnell, L.-A. and Cilliers, P. J. (2010), *GPS phase scintillation observed over a high-latitude Antarctic station during solar minimum*, Journal of Atmospheric and Solar-Terrestrial Physics, Vol. 72, No. 9-10, pp. 718–725
- Niu, F. (2012), *Performances of GPS Signal Observables Detrending Methods for Ionosphere Scintillation Studies*, 1–63 pp., Miami University, Miami, Ohio, USA.
- De Oliveira Moraes, A., Silveira Rodrigues, F., Perrella, W. J. and Paula, E. R. (2011), *Analysis of the Characteristics of Low-Latitude GPS Amplitude Scintillation Measured During Solar Maximum Conditions and Implications for Receiver Performance*, Surveys in Geophysics, Vol. 33, No. 5, pp. 1107–1131
- Phoomchusak, P., Leelarujij, N. and Hemmakorn, N. (2003), *The Deterioration of GPS Accuracy Caused by Ionospheric Amplitude Scintillation*, , pp. 2–5 via: http://www.kmitl.ac.th/satcom/publication/ecti2004_3.pdf
- Spogli, L. and Alfonsi, L. (2009), *Climatology of GPS ionospheric scintillations over high and mid-latitude European regions*, Annales Geophysicae, Vol. 27, , pp. 3429–3437
- Tsakiri, M. (2008), *GPS processing using online services*, Journal of Surveying Engineering, No. November, pp. 115–126
- Zumberge, J., M., H., D., J., M., W. and F, W. (1997), *Precise point positioning for the efficient and robust analysis of GPS data from large networks*, Journal of Geophysical Research, Vol. 102, No. B3, pp. 5005–5017

Biography

Zhizhao Liu currently is an Assistant Professor at Department of Land Surveying and Geo-Informatics, The Hong Kong Polytechnic University. His research interests include new algorithm development for precise GNSS, Precise Point Positioning, and ionosphere & troposphere modelling. He received PhD degree from the University of Calgary, Canada in 2004.